Joel D. Despain and Greg M. Stock - Geomorphic history of Crystal Cave, Southern Sierra Nevada, California. *Journal of Cave and Karst Studies*, v. 67, no. 2, p. 92–102.

GEOMORPHIC HISTORY OF CRYSTAL CAVE, SOUTHERN SIERRA NEVADA, CALIFORNIA

JOEL D. DESPAIN
National Park Service, Sequoia and Kings Canyon National Park, CA 93271, USA Joel_Despain@nps.gov
GREG M. STOCK
Department of Geological Sciences, University of Michigan, Ann Arbor, MI 48109-1005 USA gstock@umich.edu

Cave development in mountainous regions is influenced by a number of factors, including steep catchments, highly variable allogenic recharge, large sediment fluxes, and rapid rates of canyon downcutting. Caves can help to quantify this latter process, provided their ages are determined. Here we investigate the history of 4.8 km long Crystal Cave, a complex, multiple level cave in the Sierra Nevada, through detailed geomorphic and geochronologic investigations. Crystal Cave is composed of six major levels spanning 64 m in elevation. The levels are comprised of large, low gradient conduit tubes, and are connected by numerous narrow, steeply descending canyon passages. Passages in the upstream end of the cave are significantly modified by collapse, while in the downstream section they are intact with an anastomotic maze overprinting. Dye tracing confirms that the cave stream originates from partial sinking of Yucca Creek to the north. Passage gradients, wall scallops, and sediment imbrication indicate that groundwater flowed consistently southeast through time, forming cave levels as bedrock incision of Cascade Creek lowered local base level. Although modern cave stream discharges are restricted to ~0.03 $m^3 s^{-1}$, likely due to passage collapse near the sink point ca. 0.5 million years ago (Ma), bedrock scallops and coarse clastic sediment in upper levels indicate paleodischarges as much as three orders of magnitude greater prior to that time. Infrequent high discharge flood events played an important role in passage development and sediment transport. Cosmogenic $^{26}Al/^{10}Be$ burial dating of sediment suggests that the majority of Crystal Cave formed rapidly between ca. 1.2 and 0.5 Ma; rates of cave development approach theoretical maximums, presumably due to a combination of allogenic recharge highly undersaturated with respect to calcite, and physical erosion by transported sediment.

INTRODUCTION

Mountainous regions impart a distinctive set of conditions that affect cave development. Among these are steep, often sparsely vegetated catchments, highly variable stream discharges, allogenic recharge undersaturated with respect to calcite, high sediment flux, and rapid rates of landscape erosion. Caves can play an important role in quantifying the topographic evolution of mountainous regions because their development is often closely tied to local base level position, which is set by the most deeply incised local stream. Provided their ages can be determined, caves in canyon walls can record rates of river incision and topographic development (e.g., Ford *et al*., 1981; Atkinson and Rowe, 1992; Sasowsky *et al.*, 1995; Farrant *et al.*, 1995; Springer *et al.*, 1997; Granger *et al.*, 1997, 2001; Stock *et al.*, 2004; Anthony and Granger, 2004). One fundamental challenge facing cave-related landscape evolution studies is reliably determining cave ages (Sasowsky, 1998; Stock *et al.*, 2005). Another challenge is discerning the history of cave development through observations, measurements, and interpretations of cave morphology. If these two challenges can be sufficiently resolved, and the resulting information integrated into a comprehensive geomorphic history, then caves can provide important constraints on the evolution of mountainous topography.

Stock *et al.* (2005) dated sediment and speleothem deposits from caves in the Sierra Nevada of California and concluded that cosmogenic $^{26}Al/^{10}Be$ burial dating of coarse clastic sediment provided the most reliable cave ages. Using the chronology provided by burial ages, we have investigated the geomorphology of Crystal Cave, a complex, multi-level system, to understand better how caves develop in mountain settings and how cave morphology relates to overall landscape evolution.

SETTING

Crystal Cave is located within Sequoia National Park, on the western slope of the southern Sierra Nevada (Fig. 1 inset). The Sierra Nevada is an asymmetric, west-tilted fault block with a mean altitude of ~2800 m and altitudes at the range crest as great as 4419 m (Bateman and Wahrhaftig, 1966; Wakabayashi and Sawyer, 2001). Below the glacially sculpted range crest, the broad western slope of the range descends in a series of undulating low relief upland surfaces punctuated by deeply incised river canyons. Most of the caves in the range have formed proximal to these rivers.

The Sierra Nevada presents a unique setting for cave forming processes. The climate of the study area is distinctly Mediterranean, with cool, wet winters and hot, dry summers. Groundwater recharge for Sierra Nevada caves is typically allogenic, derived from sinking streams that originate in granitic catchments. These drainages are often steep and may drop several thousand meters over very short (10–30 km) distances. Much of the precipitation in the southern Sierra Nevada falls in the winter as snow. Increasing spring temperatures lead

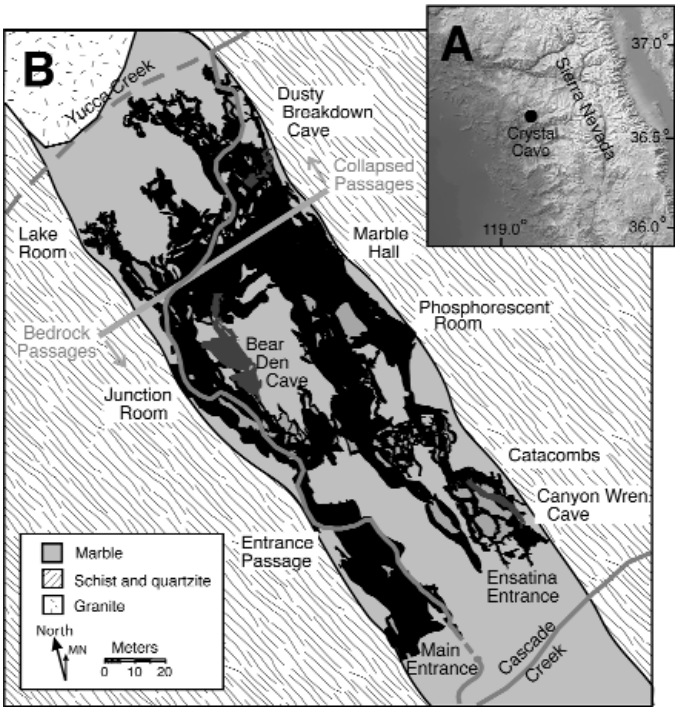

Figure 1. A: Location of Crystal Cave in the southern Sierra Nevada. B: Plan view of the cave showing passage layout, hydrology, and geology. Satellite caves shown in dark gray; streams shown by light gray lines, dashed where intermittent or inferred. Geology modified from Sisson and Moore (1994).

to dramatic seasonal run-off with stream discharges rising two or even three orders of magnitude over the course of days to weeks. Less frequent but much larger floods, resulting from unseasonably warm rainfall onto a dense snow pack, augment these annual floods. Recent events of this nature have occurred within the study area in 1957, 1969, 1997 and 2002. Because of the steep granitic catchments that supply water to Sierra Nevada caves, and the dominance of sinking stream recharge and flooding, sediment flux through cave passages is high, complicating cave conduit development.

Crystal Cave and adjacent small satellite caves sit at elevations ranging from 1386 to 1446 m, and occupy the lower 64 m of a marble ridge approximately 160 m long and 40 m wide (Fig. 1). Within this narrow ridge there are 4.87 km of surveyed cave passages. The extent of cave passages and the small size of the marble lens have produced a high percentage of voids within the bedrock, ~11%. The cave and ridge lie between Yucca and Cascade creeks, two tributaries of the North Fork of the Kaweah River. In the vicinity of Crystal Cave, these streams have incised as much as 250 m into the surrounding bedrock, forming deep canyons with steep (up to 55°) hillslopes. Although located near the western limit of Pleistocene glaciation, these drainages remained ice-free during glacial periods (Matthes, 1965), so their rugged relief is solely a product of stream incision.

GEOLOGIC AND STRUCTURAL CONTROLS ON CAVE DEVELOPMENT

Crystal Cave has formed within marble of the Sequoia pendant, one of many metamorphic pendants trending northwest across the Sierra Nevada. The Sequoia pendant is composed primarily of Jurassic and/or Triassic quartz-biotite schist interlayered with quartzite, but includes tabular masses of coarse-grained marble (Sisson and Moore, 1994). A general northwest trend of these rocks is evident despite strong deformation; beds typically strike northwest (~320°) and are nearly vertically oriented (~87° SW). The Sequoia Pendant is approximately 27 km long and 2 km wide, and is surrounded by Jurassic and Cretaceous plutonic rocks of the Sierra Nevada Batholith (Sisson and Moore, 1994). Crystal Cave has formed in a narrow lens of coarsely crystalline, vertically bedded marble. This lens is never more than 60 m wide, though it extends in a northwesterly orientation for nearly 2 km. The marble lens is bounded on both the northeast and southwest by biotite-feldspar-quartz schist (Fig. 1). Numerous thin (0.1–2 m) interbeds of schist and quartzite are present within the marble.

Most passages in Crystal Cave have developed on strike, parallel to the axis of the marble lens and the metamorphic pendent (Fig 1). Many cave walls are composed of schist, particularly along the margins of the cave, and these contacts provided the primary porosity for passage development.

DESCRIPTION OF CAVE PASSAGES

During a three-year-long effort, and with the help of many volunteers, we surveyed Crystal Cave using compasses, clinometers and fiberglass tapes. Fore- and back-sight readings along major routes and between entrances produced surveys with less than 1% error. Resurveys of poor loop closures (>2 standard deviations) in smaller passages and minor routes produced a total survey error of less than 2%. Crystal Cave currently stands at 4.77 km long, while adjacent Bear Den, Dusty Breakdown, and Canyon Wren caves are 46, 25, and 27 m long, respectively (Fig. 1).

The Crystal Cave system is composed of six distinct levels (the term "level" here refers to a specific phase of cave development and does not imply a lack of passage gradient). The levels have a combined vertical relief of 64 m (Fig. 2). Four of the levels contain the largest passages in the cave, primarily large, low gradient tubes and wide canyons (Oberhansley, 1946). Two levels have smaller passages and are shorter in length with more prominent vadose incision in passage floors. Steep, narrow, meandering vadose canyons connect all but one of the levels (Fig. 2).

The highest levels of the cave lie preferentially near the eastern, upstream edge of the marble, and subsequent lower levels show a progressive shift of cave development toward the western, downstream edge of the marble (Fig. 3). The lowest level of the cave contains a perennial stream. In the northern upstream portion of the cave extensive breakdown collapse is superimposed upon previously intact passages. The col-

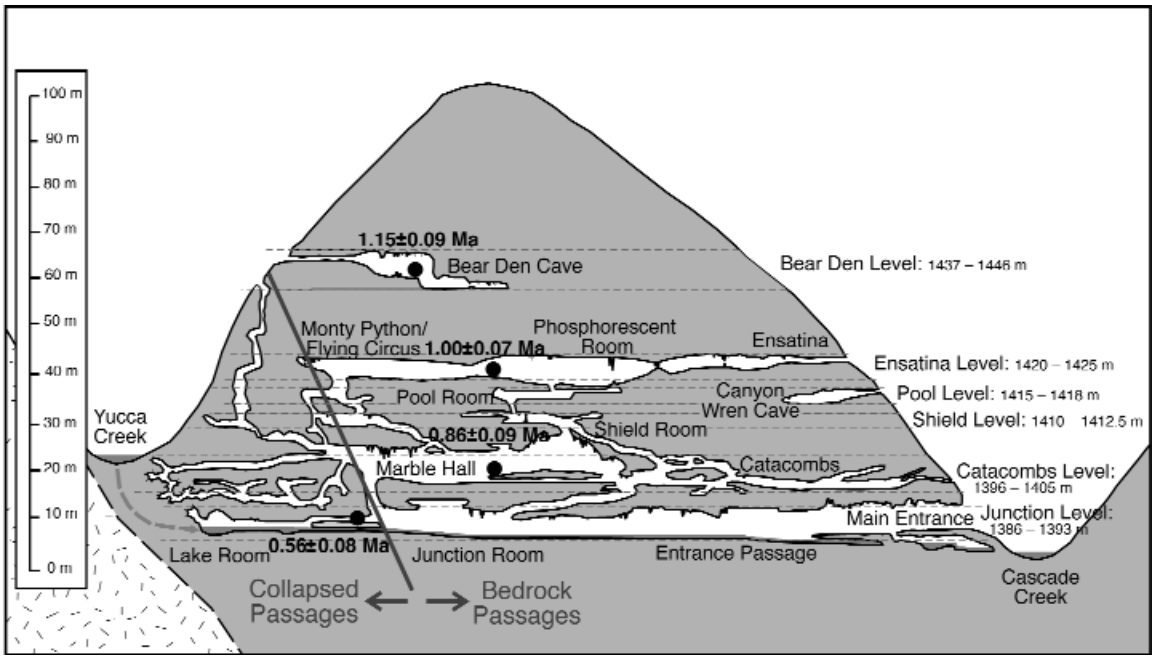

Figure 2. Profile view of Crystal Cave and surrounding caves showing pronounced cave levels. Highest level cave (Bear Den) formed first, while lowest level (Entrance Passage) contains an active vadose stream and several shallow phreatic pools. Vertical development of cave levels is controlled by incision rate of Cascade Creek; this rate is constrained by cosmogenic $^{26}Al/^{10}Be$ burial dates for coarse clastic sediments shown by black circles (Stock *et al.*, 2005).

lapsed area extends from base-level pools in the lowest sections of Crystal Cave to the overlying hillslope (Fig 2). Collapsed areas include Dusty Breakdown Cave and the northernmost 65 m of Crystal Cave, north of the Fault Room (Fig. 1).

The uppermost level of the cave system, the Bear Den level (Fig. 2), consists of a small upper canyon 0.3–0.5 m wide and 2–3 m tall and a lower section of broad rooms 3–10 m wide. Below the Bear Den level is a 12 m vertical gap in passage development. The next highest level, the Ensantina level, is a low-gradient passage containing the large Phosphorescent Room, 8 m wide and 4 m tall. Much of the Ensatina Passage lies along the eastern margin of the marble (Fig. 3). The upstream end of the Phosphorescent Room terminates in a large choke of sediment covered with flowstone. Two parallel and interconnected canyons (the Monty Python and Flying Circus passages) bifurcate from the northwest end of the Phosphorescent Room at a non-graded intersection. Four steep, narrow canyons approximately 1 m tall and 0.5 m wide connect the Ensatina level to the smaller Pool Room level below (Fig. 2). The relatively small Pool Room and Shield Room are distinguished from their connecting slot canyons by their very low gradients and broad cross sections. Although the downstream end of the Pool Room level terminates in flowstone, Canyon Wren Cave, 40 m to the southeast, is the apparent continuation of this level. Two steep slot canyons connect the Pool level to the Shield level, and five such canyons connect the Shield Room level to the lower-lying Catacombs level. The Catacombs level contains the most extensive development within the cave system, including Marble Hall (the largest room in the cave), the Dome Room, the Organ Room, the Cathedral and Junction balconies, the Catacombs, and

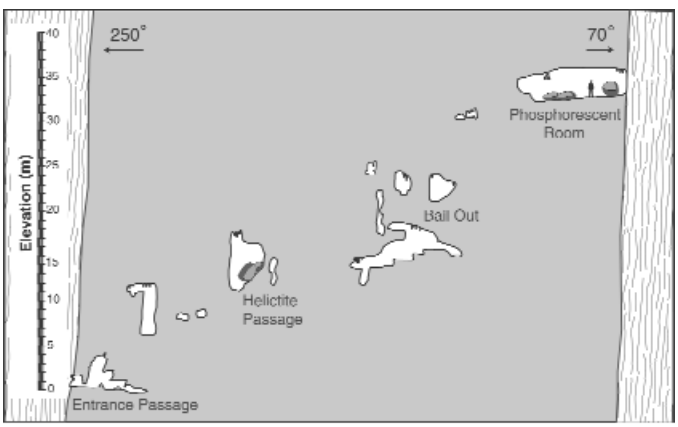

Figure 3. Cross-section view through Crystal Cave passages, normal to north-northwest trend of cave, showing progressive shift of cave development toward western, downstream edge of marble.

numerous adjacent passages. The complex anastomotic mazes of the Catacombs make up the downstream terminus of this level of the cave adjacent to the Cascade Creek canyon. The Organ Room/Curtain Room area constitutes one of only two sections of the caves that developed perpendicular to strike, across the marble lens. The other passage, the Fault Room, is an enlarged fracture parallel to and at the margin of northern collapsed sections of the caves. Canyons connecting the Catacombs level to the lowest Junction level vary from gently dipping to vertical slots. The Junction level consists primarily of the large Entrance Passage, which is up to 6 m wide and 6 m tall and contains the active cave stream.

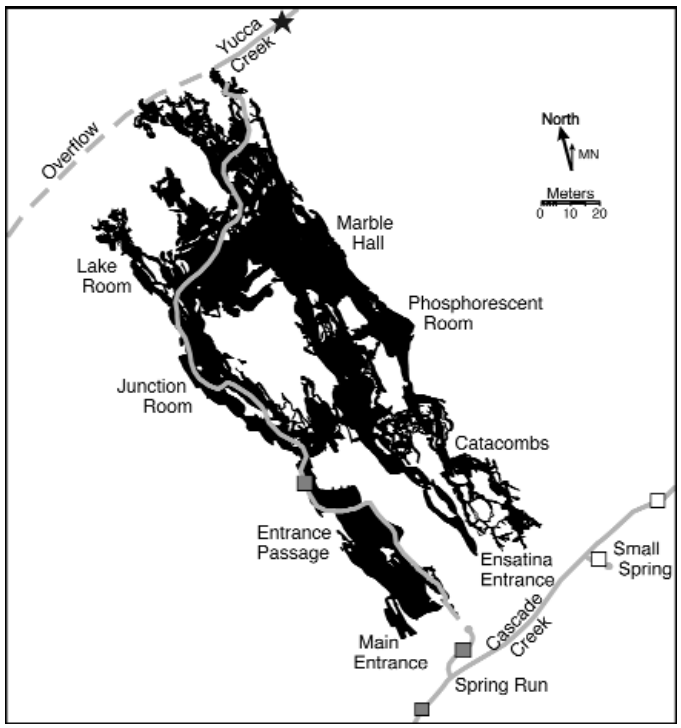

Figure 4. Plan view of Crystal Cave showing streams, locations of dye receptors, and results of dye trace experiment. Cave and surface streams shown by gray lines, dashed where intermittent. White squares show the locations of receptors that did not contain dye, and gray squares mark locations of receptors showing dye within 24 hours after the dye injection. Star indicates location of dye injection point.

PRESENT HYDROLOGIC SETTING

The active cave stream first appears in the northern portion of the cave through breakdown and subsequently flows through the large Entrance Passage to emerge in front of the Spider Web Gate Entrance as a small spring (Fig. 4). To test our assumption that the cave stream derives from sinking of Yucca Creek, we conducted a qualitative dye trace. We used dye receptors of ~10 g of activated coconut husk charcoal contained within mesh netting, and positioned them at various sites within the Crystal Cave hydrologic system (Fig. 4). We then injected 2 L of Rhodamine WT dye into Yucca Creek approximately 40 m upstream from the sink point. The following day we collected the receptors and, after rinsing with water and drying, eluted the dye with ~50 ml of 10% ammonium hydroxide in 50% aqueous 1-propanol solution (Smart and Brown, 1973). The dye trace produced positive results in three locations: (1) Yucca Creek downstream from the cave, (2) the cave stream, and (3) below the cave stream resurgence (Fig. 4). This test confirms that the cave stream originates from Yucca Creek. Transit time through the cave was less than 24 hours, suggesting that water storage within the cave is minimal.

Surface streams in the Sierra Nevada experience considerable seasonal and annual fluctuations in discharge, largely dependent on the amount of snow pack and rapidity of melt. However, the Crystal Cave stream presently appears to be immune to such discharge fluctuations. For example, we measured the discharge of the cave stream during 1994, a relatively dry year with only 48% of mean annual precipitation, and again in 1995, a wet year with 270% of mean annual precipitation. Discharge in early May of 1994 was 0.028 $m^3\ s^{-1}$, and by September had dropped to 0.012 $m^3\ s^{-1}$. Despite markedly greater precipitation, stream discharges in 1995 were similar to those in 1994. Discharge in mid-May of 1995 was 0.031 $m^3\ s^{-1}$, and dropped to 0.014 $m^3\ s^{-1}$ in September. The surprisingly small variance reveals that factors other than precipitation amount and runoff control discharge of the cave stream. Collapse and passage blockage in the northern, upstream sections of Crystal likely allowed a mantle of granitic sediments and landslide debris to constrict the sink area, limiting recharge into the cave. During times of low discharge, generally July through October, all of Yucca Creek diverts underground, while during times of high discharge, November to June, much of the flow remains on the surface (Fig. 4).

PALEOHYDROLOGY

Asymmetric bedrock scallops on cave surfaces can be used to infer both paleoflow direction and velocity (Curl, 1974). We examined 222 scallops at 17 locations within the major levels of the cave to understand better the paleohydrologic regimes that formed these passages. Measured scallops were selected based on abundance (i.e., the number of scallops present at a site) and the presence of distinct scallop margins needed for precise measurements. Scallop lengths were measured across their greatest length, and width measured normal to the length. Scallop orientations consistently show that the present pattern of water flow through the cave (from Yucca Creek to Cascade Creek) persisted throughout the duration of cave development. This observation is corroborated by both ceiling and floor gradients of major passages that dip from Yucca Creek toward Cascade Creek, and by occasional imbrication of coarse sediments within these passages.

Curl (1974) demonstrated a relation between mean scallop length, L, and the Reynolds number, Re_L, for scallops in both parallel wall and circular conduits. We determined mean scallop lengths for each set of scallop populations and used Curl's (1974) predicted relation between Reynolds number and the ratio of conduit width, D, to mean scallop length, L, in parallel wall conduits to determine Re_L values for each site. We then used the relation between L and Re_L to calculate mean flow velocity, v, through these conduits using the relation:

$$v = \upsilon \frac{\overline{Re_L}}{\overline{L}} \quad (1)$$

where υ is the kinematic viscosity (~0.013 $cm^2\ s^{-1}$ for fresh

water at 10°C; Curl, 1974). Scallop lengths indicate reasonable paleoflow velocities ranging from 0.05 to 0.96 ms^{-1} (Table 1). Multiplying flow velocities by passage cross-sectional areas yield paleodischarges at these sites that span two orders of magnitude, ranging from 0.12 to 15.19 m^3s^{-1} (Table 1). As a first order approximation, scallop measurements imply extremely variable discharges, presumably due to flood events, a common occurrence in steep mountainous catchments. This finding is in general accord with those of Lauritzen *et al.* (1983, 1985) who found that modern scallops in Norwegian caves preserved flood discharges three times larger than mean annual discharges. However, a potentially serious complication inherent to scallop-based discharge calculations is that passage cross-sectional areas may have enlarged considerably after scallops formed; thus, although the flow velocities determined from scallops may be accurate, calculated discharge values may be too large. In fact, we see abundant evidence for vadose enlargement of many passages after their initial development (see below).

To check the accuracy of the scallop-based paleodischarges, we used an independent method for determining paleodischarges in these passages based on the size of clastic sediment particles. Sediment particles of a certain size require a critical shear stress generated by the flow to entrain them. For spherical particles, the relationship between critical shear stress, τ_c, and particle size, d, is described by the Shields equation (Shields, 1936):

$$\tau_c = \beta(\rho_p - \rho_f)gd \quad (2)$$

where β is the Shields function (0.056 for typical gravel beds), ρ_p is the particle density (2700 kg m^{-3}), ρ_f is the fluid density (1000 kg m^{-3}), g is gravitational acceleration (9.81 m s^{-2}), and d is the sediment particle diameter in meters. We examined 63 sediment particles at 19 sites. At each site, we measured the population of largest spherical particle diameters, which best represent the maximum discharge conditions before the basal shear stress of the flow fell below the critical shear stress necessary to transport the particles. We then used τ_c values to calculate the critical flow depths, h_c, required to entrain the particles, using an expression for basal shear stress (Bagnold, 1966):

$$\tau_b = \rho_f g h_c S \quad (3)$$

where S is the local passage slope. We determined passage slopes by averaging over a length of ~30 m up and down passage from the sample sites; when possible, we used the slope of passage ceilings rather than floors, which are uneven due to accumulations of sediment and breakdown. We determined critical flow velocities, U_c, by combining the critical flow depths with two different methods for estimating the flow resistance. The first method uses a friction factor, f, which is a function of the Reynolds number and the relative conduit roughness:

$$U_c = \frac{\sqrt{8gh_cS}}{f} \quad (4)$$

where f is the friction factor, assumed to be 0.05, a value typical for turbulent flow in most cave conduits (Palmer, 1987). The second method of calculating the critical flow velocity utilizes a flow resistance based on hydraulic radius:

$$U_c = \frac{R_H^{0.66} S^{0.5}}{n} \quad (5)$$

where R_H is the hydraulic radius, determined using passage width and the critical flow depth calculated from Eq. 3. The variable n is known as Manning's roughness coefficient, and is defined as:

$$n = 0.32 S^{0.38} h_c^{-0.16} \quad (6)$$

Again, we multiplied the critical flow velocities calculated by these two methods (friction factor f and Manning's n) by passage cross-sectional areas to derive maximum paleodischarges (Table 2). As with those based on scallops, the paleodischarges we calculate from sediment clast sizes are quite variable, ranging from 0.01 to 39.1 $m^3\ s^{-1}$. All but one of these paleodischarges are greater than the present maximum stream discharge of ~0.03 $m^3\ s^{-1}$. This is expected because most of the sediment clasts we used to calculate paleodischarges are larger than those in the active cave stream channel, and our observations indicate that even these smaller clasts are not being transported by the present low stream flow. Even when the considerable uncertainty in the paleodischarge measurements is taken into account, the large (up to 20 cm) sediment clasts in rooms such as the Phosphorescent Room demand much higher discharges than the present stream flow to transport them. Thus, there is considerable evidence implicating infrequent but very large discharge events in the dissolution and sedimentation of the cave. Greater discharges in the past likely reflect changing climatic conditions; the present warm and dry Holocene climate of the Sierra Nevada differs markedly from the cooler, wetter climates of glacial times that dominated most of the past ~2 Myr (e.g., Benson and Thompson, 1987; Hostetler and Clark, 1997; Bartlein *et al.*, 1998; Clark *et al.*, 2003). Paleodischarges recorded by scallops and sediment clasts likely occurred during large floods that caused cave passages to enlarge rapidly.

PHREATIC AND VADOSE DEVELOPMENT

In the absence of horizontal structural control, as is generally the case in vertically bedded rock, large, low-gradient passages are thought to form at or near the piezometric surface. The piezometric surface marks the position of the water table and therefore the transition between phreatic and vadose cave

Table 1. Flow velocities and discharges for Crystal Cave passages deduced from bedrock scallops.

Location	L[a] (m)	Conduit width (m)	D/L ratio[b]	Reynolds number[c]	Flow velocity (m s^{-1})	Cross-sectional area (m^2)	Discharge (m^3 s^{-1})
Ensatina Entrance	0.108	1.25	11.6	0.0250	0.303	2.08	0.63
Ensatina constriction 1	0.483	1.4	2.9	0.0190	0.051	2.29	0.12
Ensatina constriction 2	0.200	1.3	6.5	0.0210	0.137	2.01	0.28
Ensatina Passage ceiling	0.380	2.1	5.5	0.0205	0.071	5.08	0.36
Pool Room	0.084	0.7	8.3	0.0230	0.358	3.05	1.09
Pool Room	0.065	0.8	12.3	0.0250	0.503	3.76	1.39
Monty Python Passage	0.051	0.6	11.8	0.0250	0.641	1.01	0.64
Marble Hall Overlook	0.061	1.4	23.0	0.0285	0.611	2.63	1.60
Fat Man's Misery	0.055	0.4	7.3	0.0220	0.523	13.50	7.06
Catacombs Corridor	0.310	1.5	4.8	0.0200	0.084	15.87	1.34
Catacombs Corridor	0.043	1.7	39.5	0.0315	0.957	15.87	15.19
Catacombs Red Belly	0.136	0.7	5.1	0.0205	0.197	8.37	1.65
Catacombs Hedlund Complex	0.072	0.6	8.3	0.0230	0.418	2.87	1.20
Entrance Passage	0.124	4.7	37.9	0.0300	0.316	30.25	9.57
Entrance Passage	0.093	3.8	40.9	0.0305	0.429	16.35	7.01
Entrance Passage	0.086	7.0	61.4	0.0375	0.570	16.35	9.32
Entrance Passage	0.065	7.1	109.2	0.0380	0.764	16.35	12.49

[a] Mean scallop length for the population of scallops.
[b] Conduit width to mean scallop length
[c] Determined from relations of Curl (1974), assuming parallel wall conduits.

development. It is determined by the position of the most deeply incised local surface stream (Palmer, 1987). In classic models, large, low gradient passages are often portrayed as having formed along this surface, i.e., having a shallow phreatic origin (e.g., Ford and Ewers, 1978; White, 1988; Ford and Williams, 1989; Palmer, 1991). While undoubtedly many of the low-gradient passages in Crystal Cave did form in such conditions, we suspect that several of the large, low gradient passages reflect vadose, or at least paraphreatic (alternating vadose and phreatic) development, produced during the flood-induced re-establishment of conduit-filling phreatic conditions. Vadose features such as wall notches are found along passage walls from floor to ceiling (Figs. 5, 6) implying sediment retention for extended periods of time and either a low gradient vadose origin or strong vadose overprinting onto tubes formed in shallow phreatic conditions.

Keyhole-shaped passages are often taken to imply a developmental history of phreatic initiation followed by vadose incision (White, 1988; Ford and Williams, 1989). However, the morphology of keyhole passages varies greatly, and in Crystal Cave may point to other processes. In Crystal Cave, most canyons, such as the Flying Circus and the Catacombs Corridor, exhibit an even width from top to bottom. However, keyhole morphologies are found in the Catacombs, in steep canyons above and below the Shield Room Level, and possibly in the Monty Python Passage. The upper sections of these keyholes are less than 50% wider than the canyons below, and the passages remain steep, even at their ceilings. The sinuous top of the Monty Python passage widens to the outside of passage curves, implying development through vadose incision. Parallel passages with the same elevations generally form simultaneously, and the Python and Flying Circus passages are free of significant breakdown and secondary formations. The development of these passages and the unusual rising ceiling downstream in Monty Python may be explained by sediment aggradation and flooding forcing ground water into parallel routes, creating a paraphreatic environment. In other passages, such as the Ensantina Passage, widening at the ceiling is in the form of obvious vadose cuts

Figure 5. Wall notches in the Entrance Passage near the Main Entrance. Although low gradient and rounded cross-section of this passage suggest shallow phreatic development, extensive wall notches suggest significant, perhaps even dominant, vadose origin. Photograph by Shane Fryer.

Table 2. Flow velocities and discharges for Crystal Cave passages based on sediment clast size.

Location	Passage slope	Clast size (m)	Critical shear stress (N m^{-2})	Critical flow depth (m)	Velocity based on f [a] (m s^{-1})	Velocity based on n [b] (m s^{-1})	Discharge based on f (m^3 s^{-1})	Discharge based on n (m^3 s^{-1})
Ensatina Entrance	0.001	0.005	9.1	0.46	0.85	1.89	0.49	1.09
Ensatina constriction 1	0.001	0.042	45.3	3.88	2.47	2.87	13.41	15.57
Ensatina constriction 2	0.001	0.090	81.6	8.32	3.61	3.08	39.06	33.31
Ensatina Passage	0.020	0.090	81.6	0.42	3.61	3.76	3.15	3.29
Phosphorescent Room	0.020	0.195	181.3	0.90	5.32	7.08	21.56	28.70
Pool Room	0.010	0.020	18.1	0.18	1.70	1.46	0.22	0.19
Pool Room	0.010	0.020	18.1	0.18	1.70	1.60	0.25	0.24
Monty Python Passage	0.070	0.010	9.1	0.01	1.20	1.09	0.01	0.01
Marble Hall Overlook	0.011	0.045	45.3	0.38	2.55	2.63	1.35	1.39
Blue Passage	0.002	0.080	72.5	3.70	3.41	1.34	5.04	1.98
Catacombs Corridor	0.060	0.095	86.1	0.15	3.71	2.90	0.81	0.64
Catacombs Corridor	0.060	0.095	86.1	0.15	3.71	3.16	0.92	0.78
Catacombs Red Belly	0.005	0.109	98.8	2.01	3.98	1.97	5.61	2.78
Catacombs Hedlund Complex	0.040	0.009	8.2	0.02	1.14	1.10	0.01	0.01
Junction Balconies turnoff	0.100	0.050	45.3	0.05	2.69	4.34	0.41	0.66
Entrance Passage	0.025	0.040	36.3	0.15	2.41	5.61	1.74	4.06
Entrance Passage	0.010	0.030	27.2	0.28	2.09	4.82	2.20	5.08
Entrance Passage	0.010	0.030	27.2	0.28	2.09	7.24	4.05	14.05
Entrance Passage	0.010	0.030	27.2	0.28	2.09	7.31	4.11	14.39

[a] The friction factor, f, is assumed to be 0.05 (Palmer, 1987).
[b] Manning's roughness coefficient, n, determined using Equation 7.

and horizontal notches. We suspect that the development of keyhole passages may have been encouraged by the actions of vadose and paraphreatic floodwaters in concert with heavy sediment loads or other mechanisms for constricting open conduits; in this case their presence does not necessarily indicate phreatic initiation of passage development followed by vadose incision.

CAVE SEDIMENTS AND SEDIMENTATION

Clastic sediments are abundant in all levels of Crystal Cave (Oberhansley, 1946). Sediment deposits are typically clast-supported, poorly sorted gravels and cobbles in a sandy matrix; clast imbrication is generally uncommon. Clasts are predominantly composed of schistose, quartzite, and granitic lithologies. Silt and clay-sized particles are often found as capping layers and as matrix deposits between larger clasts. Exposed sediment sections range from a few centimeters to up to 5 m thick; some passages terminate in sediment fill. Remnant pockets of sediment are preserved in alcoves high on cave walls (Fig. 7). The various coarse-grained, poorly sorted, and voluminous sediment deposits suggest rapid sedimentation that periodically aggraded cave passages.

Secondary bedrock features, such as notches, ceiling channels, and pendants, suggest that certain passages experienced sediment aggradation for long time periods. Notches in passage walls form as low discharge cave streams meander across sediment-mantled channels (White, 1988). At low discharge, sediment transport is limited and the sediment protects bedrock from physical erosion. Yet the stream retains its ability to chemically erode bedrock, and incises horizontally into the wall where it runs against it. As meanders grow, their outer bends incise farther back into the walls, resulting in low, wide arcuate notches (Fig. 6). Wall notches are often mantled with fluvial sediment left after subsequent incision (Fig. 7). In other caves, wall notches whose ages correlate with interglacial peaks in global $\delta^{18}O$ curves suggest aggradation events in

Figure 6. Clastic sediments stranded within a wall notch near Marble Hall. Following notch creation in response to sediment aggradation, renewed incision formed underlying passage, leaving sediments stranded in notch. Photograph by Steven M. Bumgardner.

Figure 7. Coarse clastic sediments in an alcove in Dome Room of Crystal Cave. Photograph by Steven M. Bumgardner.

phase with global climate events (Farrant *et al.*, 1995). However, notches in Crystal Cave are clearly too numerous to relate to such large-scale climatic fluctuations. Instead, they likely formed during shorter-term aggradation events restricted to Crystal Cave.

Why did passages aggrade? Sediment aggradation in fluvial systems is generally assumed to have climatic and/or tectonic implications (e.g. Bull, 1991). Although cave sediments can plausibly record such events, interpretation of aggradation events in caves is considerably more complicated. Independent of both climate change and tectonics, variation in rates of cave sediment deposition and erosion may be affected simply by breakdown, entrance collapse, or other barriers that can sieve sediments to varying degrees or dam them entirely for long periods. Likewise, mass wasting and sinkhole creation events on the surface further influence cave sedimentation rates. However, we consider episodic large flood events, which mobilize and rapidly transport sediment, to be the most likely source of sediment aggradation in Crystal Cave passages.

Evidence from the Catacombs section of Crystal Cave (Fig. 1) supports the prevalence of previous high discharges accompanied by sediment aggradation. This area is a braided, curvilinear, anastomotic maze of now abandoned fossil passages formed on several sub-levels with a vertical extent of 11 m. Anastomotic mazes, common in Sierra Nevada caves, form when groundwater discharge overwhelms existing conduits, creating alternative flow routes (Palmer, 1975; Palmer, 1991). Such flooding is frequent in caves situated in steep mountainous catchments. Anastomotic maze development is compounded in passages blocked or constricted by breakdown, secondary mineral deposits, or sediment fill. Unlike typical anastomotic mazes that follow horizontal porosity, such as horizontal bedding, the Catacombs are largely oriented on strike along vertical foliation. Catacombs passages are generally narrow canyons less than 2 m tall, or elliptical tubes less than 1 m in diameter. The largest and lowest passage in the labyrinth is the Catacombs Corridor, a canyon passage up to 3 m tall and 1 m wide, that lies along the western margin of the maze (Figs. 1–3). That the Corridor was the dominant master conduit for the Catacombs is supported by its comparatively larger size, its lower position, and the coarser sediment clasts relative to adjacent, interconnected conduits. Although the Catacombs passages are free of collapse and secondary speleothems, sediments completely fill some adjacent passages, and multiple wall notches attest to prior sediment deposits in now open passages. These features link sediment aggradation with impoundment of the maze-forming waters. This may be particularly true for the Hedlund complex, where two interconnected loops leave and rejoin the Corridor in a morphology that would have allowed groundwater to bypass sediment constrictions.

Recent transport of cave sediments by floodwaters has been documented in Sierra Nevada caves at or near local base level. Late on January 2, 1997, the Kaweah River flooded when a warm tropical storm melted the local snow pack, raising the discharge of the Main Fork of the Kaweah River from 142 $m^3 s^{-1}$ to 1602 $m^3 s^{-1}$ in six hours. A 150 m long passage in Wild Child Cave, situated along the Marble Fork of the Kaweah, accumulated more than 175 m^3 of sediment during the event, in deposits as thick as 3 m. Floodwaters deposited gravels and cobbles in the main passage while silts and sands accumulated in alcoves. Ten m wide rooms were completely aggraded, and passages that were once easily negotiated upright were transformed into crawlways. Conversely, during the same flood event passages in nearby Lilburn Cave were enlarged by removal of sediment. Sediment excavated from these passages exited the cave at the Big Spring resurgence and formed paired terraces along the valley walls as the flood waned. These terraces contain ~1060 m^3 of mostly fine sand (John Tinsley, pers. comm.), a minimum estimate of the sediment volume removed from the cave because additional sediment was transported farther downstream during peak discharge.

Although such high discharge events have not been recorded historically for the Crystal Cave hydrologic system, this is very likely due to a combination of the episodic nature of such events (e.g., Kirchner *et al.*, 2001), a generally warmer and drier Holocene climate (e.g., Benson and Thompson, 1987; Hostetler and Clark, 1997; Bartlein *et al.*, 1998; Clark *et al.*, 2003), and the fact that, at present, groundwater recharge is limited by passage collapse in the upstream section of the cave. Higher discharges at a time when the Yucca Creek sink point was larger likely led to the significant aggradation events evident in most cave passages.

GEOCHRONOLOGY AND RATES OF PASSAGE DEVELOPMENT

The speleothem and clastic sediment deposits in Crystal Cave were the subjects of a geochronological study in which speleothem U-Th dating, sediment paleomagnetism, and cosmogenic $^{26}Al/^{10}Be$ sediment burial dating were employed to constrain the timing of cave development (Stock *et al.*, 2005). Comparison of these dating methods revealed that $^{26}Al/^{10}Be$

burial ages were markedly older than both speleothem ages and those implied by paleomagnetism of fine sediment. This is probably because coarse sediment is deposited at base level during the waning stages of cave development, while fine sediment is often deposited in cave passages above base level during floods; drip-type calcite speleothems may begin forming any time after groundwater abandonment, and often lag cave development significantly. Thus, we consider sediment burial ages to best reflect the age of Crystal Cave passages. These ages range from 1.15 ± 0.09 Ma for the uppermost Bear Den level to 0.56 ± 0.08 Ma for the lowermost Junction level (Fig. 2). As expected, burial ages are in correct stratigraphic order, i.e., the higher cave levels are sequentially older than the lower levels.

Cosmogenic burial ages suggest that Crystal Cave development began ~1.2 Ma and proceeded rapidly until ~0.5 Ma, after which time passage development slowed markedly. That 4.72 km of cave passages spanning 64 vertical m developed in just 0.7 Myr suggests rapid rates of cave development; although direct measurements of passage widening rates is complicated by the numerous aggradational events in the cave, simple calculations suggest that widening rates approached, and in some cases even exceeded, theoretical maximums of ~1 mm yr^{-1} based on dissolution kinetics (Palmer, 1991). We consider these rapid rates to be due primarily to large volumes of chemically aggressive allogenic recharge entering the cave during floods, which can dissolve cave passages rapidly (Palmer, 2001). Passage widening was likely enhanced by physical abrasion of cave surfaces by both coarse and fine sediments entrained by these floodwaters.

Sixty-four m of vertical cave development in 0.7 Myr yields a mean Cascade Creek incision rate of 0.09 mm yr^{-1}. The intermediate dated levels provide further detail, and show a marked decrease in the rate of incision from 0.18 to 0.015 mm yr^{-1} over 0.7 Myr (Fig. 2). This pattern of decreasing incision is found in many other drainages in the southern Sierra Nevada, including Yucca Creek downstream from Crystal Cave, and is thought to reflect the waning effects of Pliocene uplift of the range (Stock *et al.*, 2004).

CONCEPTUAL MODEL OF CAVE DEVELOPMENT

A series of long-lasting conditions influenced the general development of Crystal Cave, the most influential of which has been the vertical position of Cascade Creek. Over time, bedrock incision of Cascade Creek lowered local base level, exposing cave passages to free-surface streams carrying coarse clastic sediment from Yucca Creek, particularly during floods. Due to the chemically aggressive nature of floodwaters, their ability to carry coarse sediments that promote mechanical erosion, and the prevalence of seasonal flooding and episodic extreme floods in this region, we hypothesize that pulses of rapid cave development accompanied these floods. As bedrock incision progressively lowered the Cascade Creek channel, the cave stream was pirated to lower cave levels and upper passages received sediment only during floods. Eventually, old conduits were abandoned, protecting fluvial sediments from further erosion. Subsequent deposition was limited to breakdown from the cave walls and ceilings, and accumulation of calcite speleothems from meteoric seepage.

After ~0.5 Ma, the lowering of cave passages and the development of lower levels appears to have slowed considerably. At present, there is little active dissolution of cave passages, and the only enlargement of the cave is in the vadose channel the cave stream is incising into the floor of the Entrance Passage, and potentially in phreatic pools, such as Solstice Lake. We consider two reasons for the reduction in the rate of base level lowering, and thus cave development. The first possible reason relates to restrictions on the size of the cave stream resulting from passage collapse. Extensive collapse of previously large conduits in the northern, upstream portion of the cave likely restricted cave stream discharge, greatly reducing cave development. However, the level of Cascade Creek ultimately drives cave development, so the second possible reason is that the rate of bedrock incision of Cascade Creek has slowed down since ~0.5 Ma. In a study of many other caves in the region, Stock *et al.* (2004) demonstrated a marked reduction in incision rates for many southern Sierra Nevada rivers over the last ~1 million years. Although the reasons for this slowdown are not fully understood, that this pattern is shown throughout the southern part of the range suggests that it is also a plausible mechanism for reducing the rate of cave development. Of course, these two reasons are not mutually exclusive, and both may have served to slow development of Crystal Cave over the past 0.5 million years.

In addition, we hypothesize that the incision of Cascade Creek in front of the Crystal Cave system is punctuated by the upstream migration of knickpoints. A longitudinal profile of Cascade and Yucca Creek across the vertically bedded lithologies of the Sequoia metamorphic pendant shows zones of steep channel gradients (i.e., knickpoints) within the schist and quartzite lithologies, but relatively low gradients within the marble (Fig. 8). We suspect that once knickpoints work through the resistant lithologies downstream from the cave they translate rapidly through the marble portion of the streambed, presumably due to the additional erosional influence of chemical dissolution and the greater susceptibility of carbonates with low hardness to physical erosion. This leads to a rapid drop in local base level to which the cave stream must adjust. The shallow phreatic and/or low gradient vadose passages described above are abandoned for sections of steeper, lower canyons, leading to a new, lower base level. Thus, one plausible mechanism to explain the frequent changes from large, low gradient tubular passages to narrow, steep canyons is the periodic abrupt drop in local base level associated with rapid knickpoint migration in front of the cave.

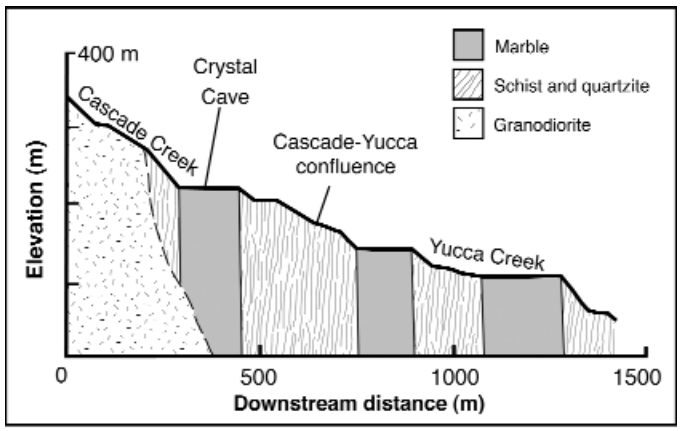

Figure 8. Longitudinal profile of Cascade Creek, and Yucca Creek below its confluence with Cascade Creek. Stepped profile, with prominent knickpoints, results primarily from contrasting vertically bedded lithologies. Channel gradients are low in relatively soft, chemically soluble marble and very steep in relatively hard, insoluble schist and quartzite. Knickpoints presumably migrate quickly upstream through marble lenses and stall on schist and quartzite, influencing local base level that controls development of Crystal Cave levels.

CONCLUSIONS

Our investigations of Crystal Cave suggest the following history of cave development:

Uppermost Bear Den level formed at ~1.2 Ma as water from Yucca Creek flowed southeast through the ridge toward Cascade Creek.

After an apparent ~200 kyr pause in passage development, but during which time Cascade Creek incised some 12 m, the Ensatina level formed at ~1.0 Ma. The Ensantina Passage and Phosphorescent Room formed first, while the parallel Monty Python and Flying Circus passages formed thereafter as a flood-deposited sediment choke in the north end of the Phosphorescent Room forced water into parallel passages.

After ~1.0 Ma, at least four small canyons developed rapidly, sequentially and headward between the Ensatina level and Pool level. The smaller Pool and Shield levels formed during apparently brief pauses in the midst of a period of otherwise rapid downward development.

Another series of small steep canyons formed below the Shield level with apparent headward migration of the active conduit.

Crystal Cave's primary level containing the Catacombs and many of the cave's largest rooms, including Marble Hall, formed at or slightly before ~0.8 Ma. The larger rooms and passages at this level may have formed due to a significant pause in the downcutting of Cascade Creek, or may reflect increased discharge as seen in scallops and sediment clasts from this level.

Collapse of the northern, upstream end of the cave ~0.5 Ma restricted input of Yucca Creek into the cave. This flow restriction, combined with decelerating Cascade Creek incision and Holocene climate change, limit present-day cave development to small phreatic pools in the upstream end of the cave and slight vadose modification of the floor of the Entrance Passage.

This detailed geomorphic history of cave development helps illustrate the unique conditions affecting cave development in mountainous regions, and provides an important context for interpreting rates of landscape evolution derived from dated cave deposits.

ACKNOWLEDGMENTS

Shane Fryer and Steve Bumgardner provided field assistance and discussions. We thank the many cavers that aided in the survey of Crystal Cave. Insightful field discussions with Darryl Granger, Arthur Palmer, Margaret Palmer, and Ira Sasowsky helped to refine many of our ideas about the geomorphic history of the cave. We acknowledge the work of Park Naturalist Frank R. Oberhansley, whose astute observations of Crystal Cave, published in 1946, were the stimulus for many of the subjects addressed in this paper.

REFERENCES

Anthony, D, and Granger, D.E., 2004, A Late Tertiary origin for multilevel caves along the western escarpment of the Cumberland Plateau, Tennessee and Kentucky, established by cosmogenic ^{26}Al and ^{10}Be: Journal of Cave and Karst Studies, v. 66, p. 46–55.

Atkinson, T.C., and Rowe, P.J., 1992, Applications of dating to denudation chronology and landscape evolution, *in* Ivanovich, M., and Harmon, R.S., eds, Uranium-series disequilibrium: Applications to Earth, Marine and Environmental Sciences, Oxford University Press, Oxford, p. 669–703.

Bagnold, R.A., 1966, An approach to the sediment transport problem from general physics: U.S. Geological Survey Professional Paper 422-I.

Bartlein, P.J., Anderson, K.H., Anderson, P.M., Edwards, M.E., Mock, C.J., Thompson, R.S., Webb, R.S., Webb III, T., and Whitlock, C., 1998, Paleoclimate simulations for North America over the past 21,000 years: Features of the simulated climate and comparisons with paleoenvironmental data: Quaternary Science Reviews, v. 17, p. 549–585.

Bateman, P.C., and Wahrhaftig, C, 1966, Geology of the Sierra Nevada, *in* Geology of Northern California, Bailey, E.H., ed.: California Division of Mines and Geology Bulletin, v. 190, p. 107–172.

Benson, L., and Thompson, R.S., 1987, The physical record of lakes in the Great Basin, *in* Ruddiman, W.F., and Wright, H.E., Jr., eds., North America and adjacent oceans during the last deglaciation: Boulder, Colorado, Geological Society of America, Geology of North America, v. K-3, p. 241–260.

Bull, W.B., 1991, Geomorphic response to climatic change: New York, Oxford University Press, 326 p.

Clark, D., Gillespie, A.R., Clark, M., and Burke, B., 2003, Mountain glaciations of the Sierra Nevada: *in* Easterbrook, D.J., ed., Quaternary Geology of the United States, INQUA 2003 Field Guide Volume, Desert Research Institute, Reno, NV, p. 287–311.

Curl, R.L., 1974, Deducing flow velocity in cave conduits from scallops: National Speleological Society Bulletin, v. 36, p. 1–5.

Farrant, A.R., Smart, P.L., Whitaker, F.F., and Tarling, D.H., 1995, Long-term Quaternary uplift rates inferred from limestone caves in Sarawak, Malaysia: Geology, v. 23, p. 357–360.

Ford, D.C., and Williams, P.W., 1989, Karst Geomorphology and Hydrology: London, England, Unwin Hyman, 601 p.

Ford, D.C., and Ewers, R.O., 1978, The development of limestone cave systems in the dimensions of length and breadth: Canadian Journal of Earth Science, v. 15, p. 1783–1798.

Ford, D.C., Schwarcz, H.P., Drake, J.J., Gascoyne, M., Harmon, R.S., and Latham, A.G., 1981, Estimates of the age of the existing relief within the southern Rocky Mountains of Canada: Artic and Alpine Research, v. 13, p. 1–10.

Granger, D.E., Kirchner, J.W., and Finkel, R.C., 1997, Quaternary downcutting rate of the New River, Virginia, measured from differential decay of cosmogenic 26Al and 10Be in cave-deposited alluvium: Geology, v. 25, p. 107–110.

Granger, D.E., Fabel, D., and Palmer, A.N., 2001, Pliocene-Pleistocene incision of the Green River, Kentucky, determined from radioactive decay of cosmogenic ^{26}Al and ^{10}Be in Mammoth Cave sediments: Geological Society of America Bulletin, v. 113, p. 825–836.

Hostetler, S.W., and Clark, P.U., 1997, Climatic controls of western U. S. glaciers at the last glacial maximum: Quaternary Science Reviews, v. 16, p. 505–511.

Kirchner, J.W., Finkel, R.C., Riebe, C.S., Granger, D.E., Clayton, J.L., King, J.G., and Megahan, W.F., 2001, Mountain erosion over 10 yr, 10 k.y., and 10 m.y. time scales: Geology, v. 29, p. 591–594.

Lauritzen, S.-E., Ive, A., and Wilkinson, B., 1983, Mean annual runoff and the scallop flow regime in a subarctic environment: Transactions, British Cave Research Association, v. 10, p. 97–102.

Lauritzen, S.-E., Abbott, J., Arnesen, R., Crossley, G., Grepperud, D., Ive, A, and Johnson, S., 1985, Morphology and hydraulics of an active phreatic conduit: Cave Science, v. 12, p. 139–146.

Matthes, F.E., 1965, Glacial Reconnaissance of Sequoia National Park, California: U.S. Geological Survey Professional Paper 504-A, 58 p.

Oberhansley, F.R., 1946, Crystal Cave in Sequoia National Park: Sequoia Natural History Association Publication, v. 1, no. 1, 32 p.

Palmer, A.N., 1975, The origin of maze caves: National Speleological Society Bulletin, v. 37, p. 56–76.

Palmer, A.N., 1987, Cave levels and their interpretation: National Speleological Society Bulletin, v. 49, p. 50–66.

Palmer, A.N., 1991, Origin and morphology of limestone caves: Geological Society of America Bulletin v. 103, p. 1–21.

Palmer, A.N., 2001, Dynamics of cave development by allogenic water: Acta Carsologica v. 30, no. 2 p. 14–32.

Sasowsky, I.D., 1998, Determining the age of what is not there: Science, v. 279, p. 1874.

Sasowsky, I.D., White, W.B., and Schmidt, V.A., 1995, Determination of stream-incision rate in the Appalachian plateaus by using cave-sediment magnetostratigraphy: Geology, v. 23, p. 415–418.

Shields, A., 1936, Anwendung der Ahnlichkeitsmechanik und der Turbulenzforschung auf die Geschiebebewegung: in Mitteilungen der Pruessischen Versuchsanstalt fur Wasserbau und Schiffbau, v. 26, 26 p. (Translated by Ott, W.P., and van Uchelen, J.C., United States Department of Agriculture, Soil Conservation Service, California Institute of Technology).

Sisson, T.W., and Moore, J.G., 1994, Geologic map of the Giant Forest quadrangle, Tulare County, California: U.S. Geological Survey Geologic Quadrangle Map GQ-1751, scale 1:62,500.

Smart, P.L., and Brown, M.C., 1973, The use of activated carbon for the detection of the tracer dye Rhodamine WT: Proceedings of the Sixth International Speleological Congress, v. 4, p. 285-292.

Springer, G.S., Kite, J.S., Schmidt, V.A., 1997, Cave sedimentation, genesis, and erosional history in the Cheat River canyon, West Virginia: Geological Society of America Bulletin, v. 109, p. 524–532.

Stock, G.M., Anderson, R.S., and Finkel, R.C., 2004, Pace of landscape evolution in the Sierra Nevada, California, revealed by cosmogenic dating of cave sediments: Geology, v. 32, p. 193–196.

Stock, G.M., Granger, D.E., Sasowsky, I.D., Anderson, R.S., and Finkel, R.C., 2005, Comparison of U-Th, paleomagnetism, and cosmogenic burial methods for dating caves: Implications for landscape evolution studies: Earth and Planetary Science Letters, v. 236, p. 388–403.

Wakabayashi, J., and Sawyer, T.L., 2001, Stream incision, tectonics, uplift, and evolution of topography of the Sierra Nevada, California: Journal of Geology, v. 109, p. 539–562.

White, W.B., 1988, Geomorphology and Hydrology of Karst Terrains: New York, Oxford University Press, 464 p.